

QUASI-STEADY AXISYMMETRIC BINGHAM-PLASTIC MODEL OF MAGNETORHEOLOGICAL FLOW DAMPER BEHAVIOR

Jin-Hyeong Yoo and Norman M. Wereley

Department of Aerospace Engineering, University of Maryland, College Park, MD 20742, USA
E-mail: jhyoo@eng.umd.edu, wereley@umd.edu

ABSTRACT

A typical magnetorheological (MR) flow mode damper consists of a piston attached to a shaft that travels in a tightly fitting hydraulic cylinder. The piston motion makes fluid flow through an annular valve in the MR damper. An electro-magnet applies magnetic field to the MR fluid as it flows through the MR valve, and changes its yield stress. An MR fluid, modeled as a Bingham-plastic material, is characterized by a field dependent yield stress, and a (nearly constant) postyield plastic viscosity. Although the analysis of such an annular MR valve is well understood, a closed form solution for the damping capacity of a damper using such an MR valve has proven to be elusive. Closed form solutions for the velocity and shear stress profile across the annular gap are well known. However, the location of the plug must be computed numerically. As a result, closed form solutions for the dynamic range (ratio of field on to field off damper force) cannot be derived. Instead of this conventional theoretic procedure, an approximated closed form solution for a dampers dynamic range, damping capacity and other key performance metrics is derived. And the approximated solution is used to validate a rectangular duct simplified analysis of MR valves for small gap condition. These approximated equations are derived, and the approximation error is also provided.

INTRODUCTION

Magnetorheological (MR) fluids are suspensions of soft magnetic particles, such as iron or cobalt, in a carrier fluid [1-3]. The benefits of such fluids are that the yield stress of the fluid can be varied through exposure to a magnetic field. MR fluids have been used in numerous types of smart actuation systems, such as dampers, clutches and isolators [4, 5]. Especially, the MR fluids are achieving success as hydraulic fluids in damping applications for military, civil and automotive systems.

The performance of the MR damper is based on the MR valve design. Most of the MR valve has a circular cross-section to construct an annular duct model because of its simple design and higher strength of the damper structure. The circular cross-

section also has an advantage of simple magnetic circuit construction. As a result, MR valves are physically realized as an annular duct. To fully account for the annular geometry of MR valves, several investigations have studied Poiseuille flow of Bingham plastic materials [6] through an annular duct. In some studies, a rectangular duct was used to approximate annular duct geometry [7,10]. Usually, the MR devices are designed using rectangular duct approximations [8] to exploit simple performance analyses.

This study focuses on determining analytical expressions for damper performance using an idealized Bingham plastic model. Dampers with cylindrical geometry are investigated, where damping forces are developed in an annular bypass via Poiseuille flow. Although the analysis of such an annular MR valve is well understood [9], a closed form solution for the damping capacity of a damper using such an MR valve has proven to be elusive. In this study, an approximate closed form solution for a damper's dynamic range, damping capacity and other key performance metrics is derived by making linear and quadratic approximations to the solution of plug location. The quadratic equation is proven to have very small error and it could be used as an analytical solution for the case where annular gap is small relative to piston radius. The approximate solution is utilized to verify rectangular duct analysis of MR valves. We will show that the approximate equivalent viscous damping coefficient (C_{eq}/C) for the annular duct reduces to that for the rectangular duct when the small gap assumption, $d/R_1 \ll 1$, is applied.

NOMENCLATURE

d	Electrode gap
Δp	Pressure drop along electrodes
r	Radial coordinate measured from shaft axis
$u(r)$	Velocity distribution in electrode gap
v_0	Piston head or shaft velocity
A	Piston head area
Bi	Bingham number
C_N	Viscous damping (Newtonian)
C_{eq}	Equivalent viscous damping (Bingham plastic)

F	Force applied to damper shaft
L	Length of inner electrode
Q	Volume flux
R_1	Outer radius of inner electrode
R_2	Inner radius of outer electrode
R_{pi}	Inner radius of plug measured from shaft axis
R_{po}	Outer radius of plug measured from shaft axis
δ	Plug thickness
$\bar{\delta}$	Ratio of plug thickness to gap
μ_0	Plastic viscosity
τ	Shear stress
τ_y	Dynamic yield shear stress

1 MR dampers

A schematic of the flow mode damper is shown in Figure 1. The annular valve formed by magnetic poles is mounted in the piston. When the piston translates, the fluid is forced through the annular valve under a pressure gradient. This design develops rate-dependent damping forces due to the pressure drop through the annular valve as force is applied to the damper shaft. The governing equation for quasi-steady valve system obtained from force equilibrium is

$$\frac{1}{r} \frac{\partial}{\partial r} (r\tau) = \frac{\partial p}{\partial z} \quad (1)$$

where τ is the shear stress, r is the radial coordinate, z is the longitudinal coordinate, and p is the pressure developed via piston head motion. We assume that p varies linearly along the length of the annular gap, so that equation (1) can be rewritten as

$$\frac{d\tau}{dr} + \frac{\tau}{r} = \frac{\Delta p}{L} \quad (2)$$

A Bingham plastic material behaves like a rigid solid below a shear stress threshold called the yield stress. This stress state is commonly called the pre-yield state. In this pre-yield state, the material is rigid and does not flow. When the shear stress exceeds the yield stress, the material behaves much like a viscous fluid. This behavior can be modeled as

$$\tau = \tau_y \operatorname{sgn}\left(\frac{du}{dr}\right) + \mu \frac{du}{dr} \quad (3)$$

Here τ_y is the dynamic yield stress and μ is the plastic viscosity. Newtonian shear flow can be viewed as a special case of Bingham plastic shear flow with zero dynamic yield stress.

2 Newtonian Model

For the flow mode damper as shown in Figure 1, applying the boundary conditions

$$u(R_1) = 0 \quad u(R_2) = 0$$

yields the velocity profile in the annular electrode gap as [9]

$$u_N = \frac{\Delta P}{4\mu_0 L} \left[R_2^2 - r^2 - \frac{R_2^2 - R_1^2}{\operatorname{Log}(R_2/R_1)} \log\left(\frac{R_2}{r}\right) \right] \quad (4)$$

where $P = P_{in} - P_{out}$. Here, P_{in} and P_{out} are the pressures at the inlet and outlet of the MR valve, respectively. The volume flux

through the electrodes, Q_N , is obtained by integrating the velocity profile over the annular electrode gap [9]

$$Q_N = \int_{R_1}^{R_2} 2\pi r u(r) dr = \frac{\Delta P \pi R_2^4}{8\mu_0 L} \left[1 - \left(\frac{R_1}{R_2}\right)^4 + \frac{(1 - (R_1/R_2)^2)^2}{\operatorname{Log}(R_1/R_2)} \right] \quad (5)$$

The volume flux through the annular electrode gap, Q_N , must equal the volume flux displaced by the piston head, Q_p , which is proportional to piston head velocity, v_0 , or

$$Q_N = Q_p = Av_0 \quad (6)$$

where A is the area of the piston head minus the area of the shaft. Substituting equation (5) into equation (6), solving for the force F , and noting that $\Delta P = F/A$ yields

$$F = C_N v_0 \quad (7)$$

where the flow mode damping can be expressed as [9]

$$C_N = 8\pi\mu_0 L \left(\frac{A}{\pi R_2^2}\right)^2 \left\{ 1 - \left(\frac{R_1}{R_2}\right)^4 + \frac{[1 - (R_1/R_2)^2]^2}{\operatorname{Log}(R_1/R_2)} \right\}^{-1} \quad (8)$$

Damping, C_N , depends only on flow mode damper geometry and off-state viscosity.

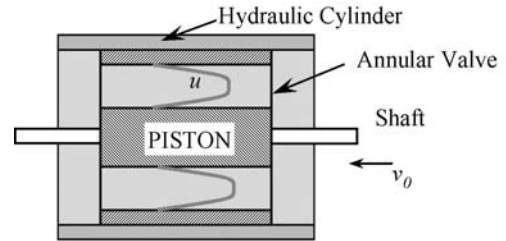


Figure 1. Schematic of fluid velocity profile through MR valve inside damper.

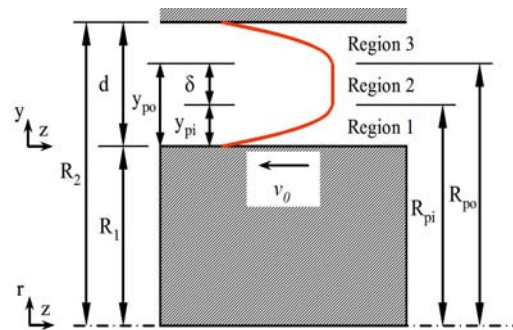


Figure 2. Coordinate systems of the MR valve for axisymmetric duct model.

3 Bingham-Plastic Model

A typical velocity profile through the annular gap for the Bingham plastic flow model is shown in Figure 2 with the coordinate system definition. The flow profile is divided into 3 regions. In the first and third regions adjacent to the valve walls, the shear stress has exceeded the yield stress and the material flows, so that these two regions represent post-yield flows. The second region or central region remains rigid, because the shear stress is lower than the yield stress, so that this region is pre-yield or plug flow. R_{pi} and R_{po} represent the inner and outer plug boundaries, respectively.

3.1 Shear Stress

The shear stress profile across the valve gap for the annular duct model, $\tau(r)$, can be determined from equation (2) as

$$\begin{aligned}\tau(r) &= \frac{R_{pi}}{r} \tau_y - \frac{\Delta P}{2L} \left(r - \frac{R_{pi}^2}{r} \right) \\ &= -\frac{R_{po}}{r} \tau_y - \frac{\Delta P}{2L} \left(r - \frac{R_{po}^2}{r} \right)\end{aligned}\quad (9)$$

From this equation, the yield stress can be expressed in terms of plug thickness, δ , as

$$\tau_y = \frac{\Delta P}{2L} (R_{po} - R_{pi}) = \frac{\Delta P}{2L} \delta \quad \text{or} \quad \delta = \frac{2L \tau_y}{\Delta P} \quad (10)$$

3.2 Velocity profile

The equation for the velocity profile is different for each region as shown in Figure 2. The volume flux through each region will be calculated separately, and summed to obtain the total volume flux through the annular electrode gap.

Region 1

The velocity at the inner electrode must equal zero since the inner electrode is stationary. The plug travels at a constant velocity, so that the velocity gradient at the Region 1 boundary adjacent to the plug must equal zero, leading to the boundary conditions

$$u(R_1) = 0 \quad \left. \frac{du}{dr} \right|_{r=R_{pi}} = 0$$

The resulting velocity profile is [9]

$$\begin{aligned}u_1(r) &= -\frac{\Delta P}{4\mu L} \left[r^2 - R_1^2 - 2R_{pi}^2 \log\left(\frac{r}{R_1}\right) \right] \\ &\quad - \frac{\tau_y}{\mu} \left[r - R_1 - R_{pi} \log\left(\frac{r}{R_1}\right) \right]\end{aligned}\quad (11)$$

Region 2

This region presents a constant plug velocity across the entire pre-yield region, from $r=R_{pi}$ to $r=R_{po}$. Plug velocity must be compatible with the velocity from Region 1 so that [9]:

$$\begin{aligned}u_2(r) &= -\frac{\Delta P}{4\mu L} \left[R_{pi}^2 - R_1^2 - 2R_{pi}^2 \log\left(\frac{R_{pi}}{R_1}\right) \right] \\ &\quad - \frac{\tau_y}{\mu} \left[R_{pi} - R_1 - R_{pi} \log\left(\frac{R_{pi}}{R_1}\right) \right]\end{aligned}\quad (12)$$

Region 3

The boundary conditions in Region 3 are similar to those for Region 1. At the edge of the plug, where $r=R_{po}$, the fluid travels at the constant plug velocity. Also, the velocity of the fluid must equal zero at the outer electrode. Thus, the boundary conditions are

$$u(R_2) = 0 \quad \left. \frac{du}{dr} \right|_{r=R_{po}} = 0$$

which leads to the velocity profile [9]

$$\begin{aligned}u_3(r) &= -\frac{\Delta P}{4\mu L} \left[r^2 - R_2^2 - 2R_{po}^2 \log\left(\frac{r}{R_2}\right) \right] \\ &\quad + \frac{\tau_y}{\mu} \left[r - R_2 - R_{po} \log\left(\frac{r}{R_2}\right) \right]\end{aligned}\quad (13)$$

There are two unknowns, R_{pi} and R_{po} , and we only have equation (10) which is related in these parameters. Another equation can be found using velocity continuity along the velocity profile through each region:

$$u_1(R_{pi}) = u_2 = u_3(R_{po}) \quad (14)$$

Traditionally, R_{pi} and R_{po} are iteratively calculated using equation (10) and (14), and then the velocity distribution in each of the three regions can be determined. However in this study, we will calculate the plug position by direct calculation of the plug center using equation (10).

3.3 Plug Center

1st approximation

Figure 3 shows plug position as a function of yield stress of an MR fluid. The solid line in this figure shows the center of plug as a function of the MR fluid yield stress. When the yield stress is zero, the plug center is given by the value of r where the Newtonian velocity profile is a maximum and it can be expressed as [11]

$$\delta_{c,N} = \delta_c(0) = \left[\frac{R_2^2 - R_1^2}{2 \log(R_2/R_1)} \right]^{1/2} \quad (15)$$

where $\delta_c(0)$ denotes the plug center in the absence of field.

As yield stress increases, the plug gradually fills in the gap. When the plug fills the gap, the plug center approaches the valve center. A linear function can be assumed to describe the plug center development with respect to the yield stress as a simple approximation. Assuming that the plug center is proportional to $\delta_{c,N}$, Eq. (15), the plug center position can be approximated as:

$$\delta_c(\tau_y) = \frac{2L}{\Delta P d} \left[\frac{R_1 + R_2}{2} - \delta_{c,N} \right] \tau_y + \delta_{c,N} \quad (16)$$

Once δ_c is calculated for a given τ_y , R_{pi} and R_{po} are calculated by

$$R_{pi} = \delta_c - \delta/2, \quad R_{po} = \delta_c + \delta/2 \quad (17)$$

Then the velocity profiles can be calculated using equations (11), (12), and (13). Thus, the velocity distribution in each of the three regions can be approximated.

2nd approximation

As can be seen in Figure 4, the plug center (dotted line) is not a linear function with respect to the yield stress. For a more precise approximation, a quadratic function is suggested to predict the plug center position as a function of yield stress. Using the boundary conditions of

$$\delta_c(0) = \left[\frac{R_2^2 - R_1^2}{2 \log(R_2/R_1)} \right]^{1/2} = \left[\frac{d(d + 2R_1)}{2 \log(1 + d/R_1)} \right]^{1/2} = \delta_{c,N}; \quad (18)$$

$$\delta_c \left(\frac{\Delta P}{2L} \right) = \frac{R_1 + R_2}{2} = R_1 + \frac{d}{2}; \quad \left. \frac{\partial \delta_c}{\partial \tau} \right|_{\tau = \frac{\Delta P d}{8L}} = 0$$

and applying a least squared error curve fit method, we can obtain an approximate quadratic equation describing the center of the plug region, δ_c , as

$$\delta_c(\tau_y) = \left(\frac{2L\tau_y}{\Delta P d} \right)^2 \left[R_1 + R_2 - 2\delta_{c,N} \right] - \left(\frac{2L\tau_y}{\Delta P d} \right) \left[\frac{R_1 + R_2}{2} - \delta_{c,N} \right] + \delta_{c,N} \quad (19)$$

where $\delta_{c,N}$ denotes the radius at which the maximum velocity occurs for Newtonian flow. Using this equation in conjunction with the plug thickness equation (10), the plug position of the axisymmetric annular duct model can be computed without resorting to a numerical root finding procedure.

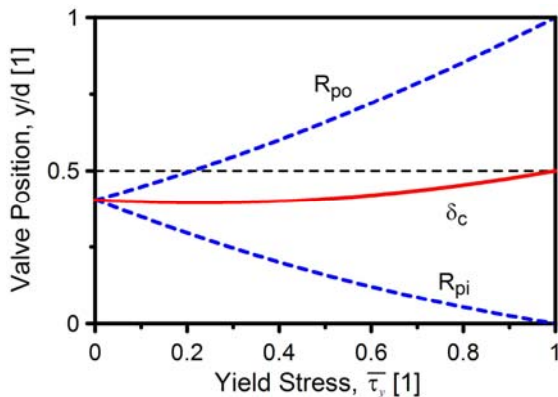


Figure 3. Plug development as a function of the yield stress for an axisymmetric annular valve.

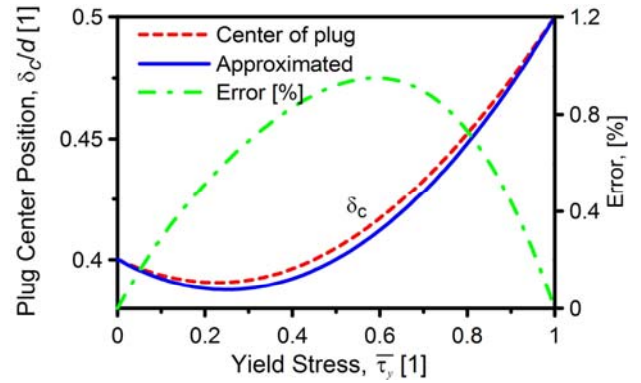


Figure 4. For the annular duct, the plug center and associated approximation error are plotted as a function of yield stress. ($d/R_1=10.0$)

3.4 Volume Flux and Damping Coefficient

The velocity of the piston is determined by equating the volume flux displaced by the piston, Q_p , to the volume flux through the annular electrode gap, Q_d , and the total volume flux is

$$Q_d = Q_1 + Q_2 + Q_3 = Q_p \quad (20)$$

where the volume flux through each region is computed via

$$\begin{aligned} Q_1 &= \int_{R_1}^{R_{pi}} u_1(r) 2\pi r dr \\ Q_2 &= \int_{R_{pi}}^{R_{po}} u_2(r) 2\pi r dr \\ Q_3 &= \int_{R_{po}}^{R_2} u_3(r) 2\pi r dr \end{aligned} \quad (21)$$

The total volume flux is then

$$\begin{aligned} Q_{a,r} &= \frac{\pi \Delta P}{24 \mu L} \left[3d^4 - 4d^3 \delta - 6d^2 \delta_c (\delta + 2\delta_c) + 3d\delta(\delta + 2\delta_c)^2 \right. \\ &\quad - \delta\delta_c(3\delta^2 + 12\delta\delta_c + 4\delta_c^2) + 6(2d^3 - 2d^2\delta - 2d\delta_c(\delta + 2\delta_c) + \delta(\delta + 2\delta_c)^2)R_1 \\ &\quad + 6(3d - 2\delta_c)R_1^2 + 4(3d - 2\delta)R_1^3 \\ &\quad + \frac{3}{4}(\delta - 2\delta_c)(\delta + 2\delta_c) \left\{ -(\delta - 2\delta_c) 2 \log \left(\frac{2\delta_c - \delta}{2R_1} \right) \right. \\ &\quad \left. \left. - 8\delta\delta_c \log \left(\frac{2\delta_c - \delta}{2R_1} \right) + (\delta + 2\delta_c)^2 \log \left(\frac{2\delta_c + \delta}{2(R_1 + d)} \right) \right\} \right] \end{aligned} \quad (22)$$

The equivalent viscous damping, C_{eq} , is given by

$$C_{eq} = \frac{A^2 \Delta P}{Q_b} = \frac{F}{v_0} \quad (23)$$

From the definition of plug thickness, Eq. (10), the Bingham number, Bi , defined as the ratio between the yield stress and the viscous stress,

$$Bi = \frac{\tau_y}{\mu v_0 / d} = \frac{A p d \delta}{2 \mu L} \times \frac{\Delta P}{Q_b} \quad (24)$$

The damping coefficient (or dynamic range) is defined as the ratio of the equivalent viscous damping, equation (23), to

the Newtonian damping, equation (8). The damping coefficient can be approximated using a Taylor series for the logarithmic function and plug center as:

$$\left(\frac{C_{eq}}{C}\right)_a \approx \frac{1 - \frac{1}{16} \left(\frac{d}{R_1}\right)^2}{\left(1 - \frac{\delta}{d}\right)^2 \left(1 + \frac{\delta}{2d}\right) \left[1 + 6 \left(\frac{d}{R_1}\right)^2\right] + \left(1 - \frac{\delta}{d}\right)^2 \left[\frac{1 - \delta}{4d}\right] \left(\frac{\delta}{R_1}\right)} \quad (25)$$

Applying a small gap assumption, that is, the valve gap, d , is much smaller than the annular radius, R_1 , the approximate damping coefficient for the axisymmetric valve simplifies to the exact solution for the rectangular duct model [10],

$$\left(\frac{C_{eq}}{C}\right)_a \approx \frac{1}{\left(1 - \delta/d\right)^2 \left(1 + \delta/(2d)\right)} \quad (26)$$

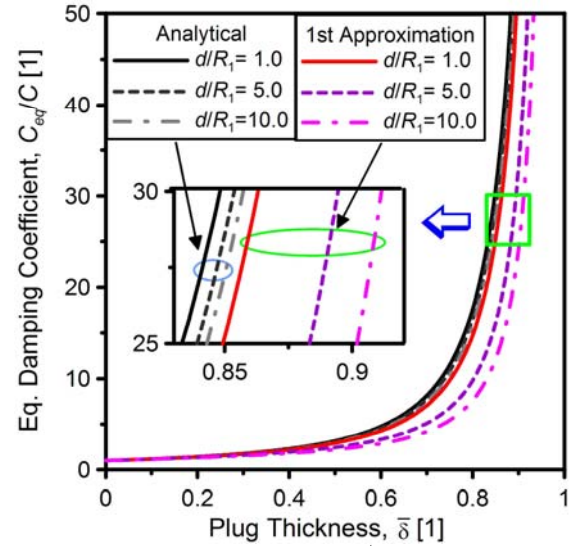
4 Analytical Results and Discussion

Figure 3 shows the plug position of the axisymmetric model as a function of the yield stress in the MR valve. In this figure, the nondimensional yield stress is defined as $\bar{\tau}_y = \tau_y / (\Delta P d / 2L)$.

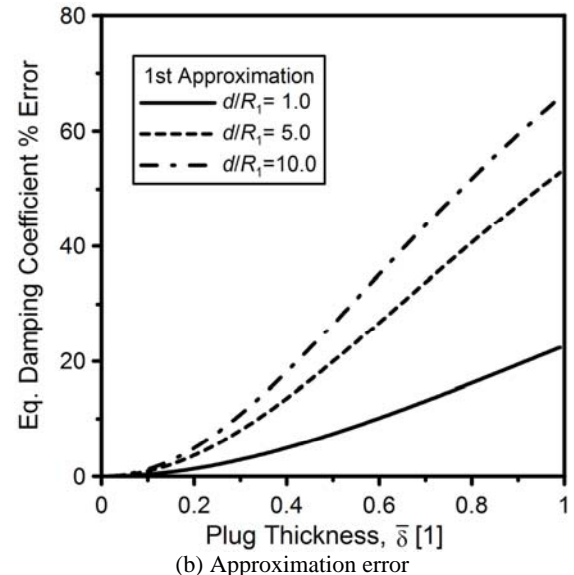
Figure 3 also shows the plug center, $\delta_c(\bar{\tau}_y) = \frac{(R_{pi} + R_{po})}{2}$

diagram with solid line. As shown in this figure, the plug center will be developed from the off-center position and the plug center gradually approaches to the center of the valve as the plug fills in the gap. Figure 4 shows the exact trajectory of the plug center development along with the normalized yield stress with fine dashed line. Even though the plug center development diagram shows a parabolic shape, a linear function is suggested as a simple approximation for plug center. This assumption gives reasonable result for a small gap range as shown in Figure 5. This result reveals that the total flow rate, which is directly related to the damping performance, is not very sensitive to the plug position. Figure 5(a) shows the 1st approximated equivalent damping coefficients versus the plug thickness comparing with the analytical solutions. In these figures, $\bar{\delta}$ is defined as a ratio between plug thickness and gap distance, δ/d . As can be seen in Figure 5(b), the maximum error level of this approximation is under 20% when the d/R_1 value is less than 1. A quadratic function can express more precise plug center trajectory along the yield stress as shown in Figure 4. Even though for the range of big gap distance ($d/R_1=10$), the plug center position error shows less than 1%. For a small gap distance range, the error level becomes a numerical error level and this approximation function can be used as an exact solution of plug center for a certain range of d/R_1 value. The equivalent viscous damping coefficient for the annular duct model with 2nd approximation method is shown in Figure 6(a). This quadratic approximation gives very precise results for the damping coefficient along with wide range of d/R_1 value as shown in Figure 6. Based on this results on Figure 6(b), the maximum error on the damping coefficient is less than 0.5%, when $d/R_1 = 1$. In a practical design of an MR damper, d/R_1 is typically 0.1, and the approximation error on the damping coefficient is about 0.001%. For the cases of $d/R_1 \ll 1$, the

approximated quadratic equation can be assumed as an analytical function for the plug center calculation.



(a) Damping coefficient with 1st approximation



(b) Approximation error

Figure 5. Comparison of equivalent viscous damping coefficients and the errors of 1st approximation for the plug center.

5. Conclusions

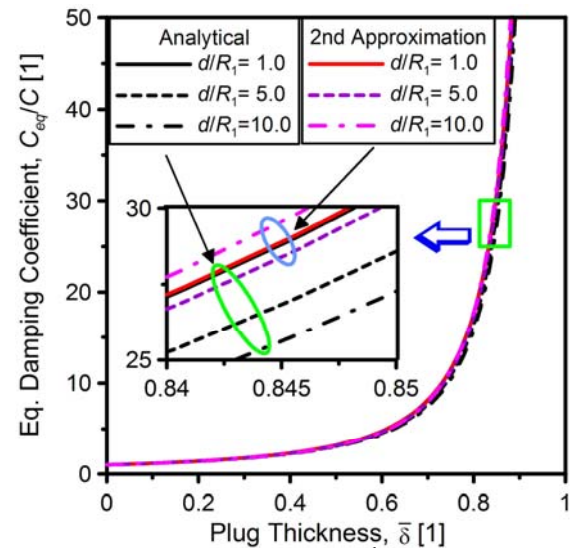
An axisymmetric quasi-steady Bingham plastic model was analyzed for an MR flow mode damper. The parametric analysis focused on flow mode damper and identified several trends of parameters and performance of the MR damper. The plug thickness and position are functions of magnetic field and applied load with yield stress of MR fluid, and the plug thickness has a substantial impact on the equivalent viscous damping levels. The approximate functions describing location of the plug center as a linear or quadratic equation simplified the calculation of the annular duct solution without resorting to numerical methods to solve the boundary value problem of

annular duct for MR valve. Especially, the quadratic equation shows very small error for the plug center calculation ($\sim 0.001\%$ of maximum error for $d/R_1=0.1$). This study shows that the equivalent viscous damping coefficient (C_{eq}/C) equation for annular duct model can be simplified to the rectangular duct model equation when a small gap assumption, $d/R_1 \ll 1$, is applicable.

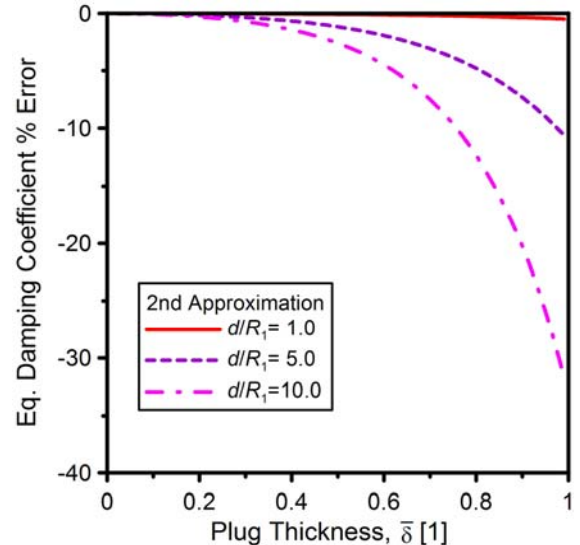
REFERENCES

1. W.I. Kordonski, S.R. Gorodkin, and Z.A. Novikova (1998). "The Influence of Ferroparticle Concentration and Size on MR Fluid Properties," *6th International Conference on Electrorheological Fluids, Magnetorheological Suspensions, and Their Applications*. World Scientific, July 22-25, 1997, pp. 535-542.
2. P.P. Phule, and J.M. Ginder (1998). "Synthesis of Novel Magnetorheological Fluids," *MRS Bulletin*, Volume 23, No. 8, August, pp. 23-25.
3. P.P. Phule, and J.M. Ginder (1998). "The Materials Science of Field-Responsive Fluids," *MRS Bulletin*, Volume 23, No. 8, August, pp. 19-22.
4. R. Stanway, J.L. Sproston, and A.K. El-Wahed (1996). "Application of Electrorheological Fluids in Vibration Control: A Survey," *Smart Materials and Structures* Vol. 5, No.4, pp. 464-482.
5. Carlson, J., Catanzarite, D. and St. Clair, K. 1996, "Commercial Magnetorheological Fluid Devices," *International Journal of Modern Physics B*, 10(23-24):2857-2865.
6. Wilkinson, W. L. 1960. *Non-Newtonian Fluids: Fluid Mechanics, Mixing, and Heat Transfer*, Pergamon, New York.
7. Bird, R.B., Dai, G.C. and Yaruso, B.J. 1983. "The Rheology and Flow of Viscoplastic Materials," *Reviews in Chemical Engineering* 1:1-70.
8. Peel, D.J., Stanway, R. and Bullough, W.A. 1996. "Dynamic Modeling of an ER Vibration Damper for Vehicle Suspension Applications," *Smart Materials and Structures*, 5(5):591-606.
9. Kamath, G.M., Hurt, M.K. and Wereley, N.M. 1996. "Analysis and Testing of Bingham Plastic Behavior in Semi-Active Electrorheological Fluid Dampers," *Smart Materials and Structures*, 5(5):576-590.
10. Wereley, N.M. and Pang, L., 1998 "Nondimensional Analysis of Semi-active Electrorheological and Magnetorheological Dampers using an Approximate Parallel Plate Model," *Smart Materials and Structures* 17:732-743.

11. White, F. M. 1986, *Fluid Mechanics*, McGraw-Hill, Inc. New York, pp.326-330.



(a) Damping coefficient with 2nd approximation



(b) Approximation error

Figure 6. Comparison of equivalent viscous damping coefficients and the errors of 2nd approximation for the plug center.